# Nanoscale

Accepted Manuscript


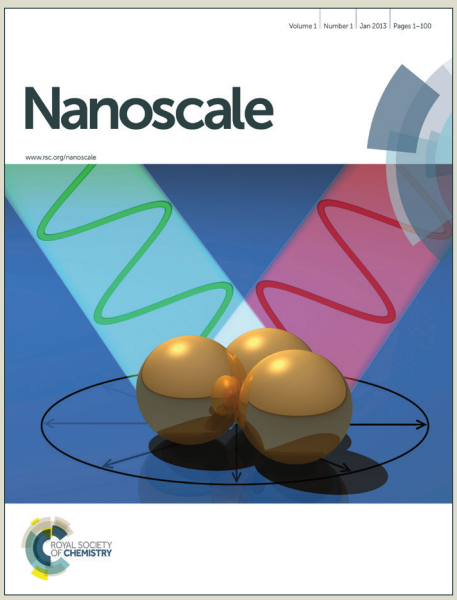





ROYAL SOCIETY OF CHEMISTRY

www.rsc.org/nanoscale

Nanoscale

RSCPublishing

COMMUNICATION

# Additive, modular functionalization of reactive self-assembled monolayers: toward the fabrication of multilevel optical storage media

Cite this: DOI: 10.1039/x0xx00000x

Received ooth January 2012,
Accepted ooth January 2012

DOI: 10.1039/x0xx00000x

www.rsc.org/

Denis Gentili[a]†, Marianna Barbalinardo[a]†, Ilse Manet[b], Margherita Durso[b], Marco Brucale[a], Alessio Mezzi[a], Manuela Melucci[b] and Massimiliano Cavallini*[a,c]

**We report a novel strategy based on iterative micro contact printing, which provides additive, modular functionalization of reactive SAMs by different functional molecules. We demonstrate that after printing the molecules form an interpenetrating network at the SAM surface preserving their individual properties. We exploited the process by fabricating new optical storage media that consist of a multilevel TAG.**

The fabrication of functional surfaces is one of the pivotal needs for many applications ranging from electronics,[1, 2] catalysis[3] to optics,[4] sensors,[5] dewetting[6, 7], thin film growth[8, 9] and bio-nanotechnology.[10, 11] A widely exploited strategy to fabricate functional and responsive surfaces relies on the fabrication of Self-Assembled Monolayers (SAMs),[12-14] which, in the last two decades, have been a crucial breakthrough for surface chemistry and that in combination with soft lithography[15, 16], have given an extraordinary contribute to the development of nanotechnology.

SAMs form by spontaneous two-dimensional organization of a precursor on a surface; functional SAMs can be achieved using functional molecular precursor, or by reacting already formed SAMs (reactive SAMs, R-SAMs)[17] with a functional molecule in a further step. Typically, spatially controlled functionalization of R-SAMs has been achieved by patterning a functional molecule then saturating the unprinted zones with a second type of molecule.[18]

Here, we report a further breakthrough in SAM technology demonstrating that iterative micro contact printing (μCP) allows additive grafting of different functional molecules in the same area of a reactive SAM, preserving molecular individual functional properties. We used the additive μCP process to fabricate a multi-level fluorescent TAG (multi-TAG), which consists of two overlapping micrometric patterns containing a digital information (e.g. Aztec code)[19]. The multi-TAG is fabricated by printing two interpenetrating fluorescent molecules that can be independently visualized. Remarkably, our approach makes possible the storage of digital information optically accessible at different level by individually accessing each pattern.

Multi-TAGs were obtained both on rigid ($SiO_2$/Si) and flexible polydimethylsiloxane (PDMS) substrates. The proposed process which exploit the consolidate technology of μCP[13], is cheap, versatile, highly reproducible and can be easily up-scaled.

In order to demonstrate the versatility of the process, we chose to use one of the most investigated R-SAMs, the one formed by (3-aminopropyl)-triethoxysilane (APTS), which is widely employed in surface chemistry applications for its ability to react efficiently with hydroxy-rich surfaces. The APTS-SAM was then chemically functionalized with two fluorescent oligothiophenes, namely bis(2,5-dioxopyrrolidin-1-yl) [2,2':5',2"-terthiophene]-5,5"-dicarboxylate, (**1**) and bis(2,5-dioxopyrrolidin-1-yl) 5,5'-(benzo [1,2,5]thiadiazole-4,7-diyl)bis(thiophene-2-carboxylate) (**2**) bearing succinimidyl-ester ends that can be coupled to amino groups of the APTS-SAM (Fig. 1a, synthesis and characterization are described in ESI).

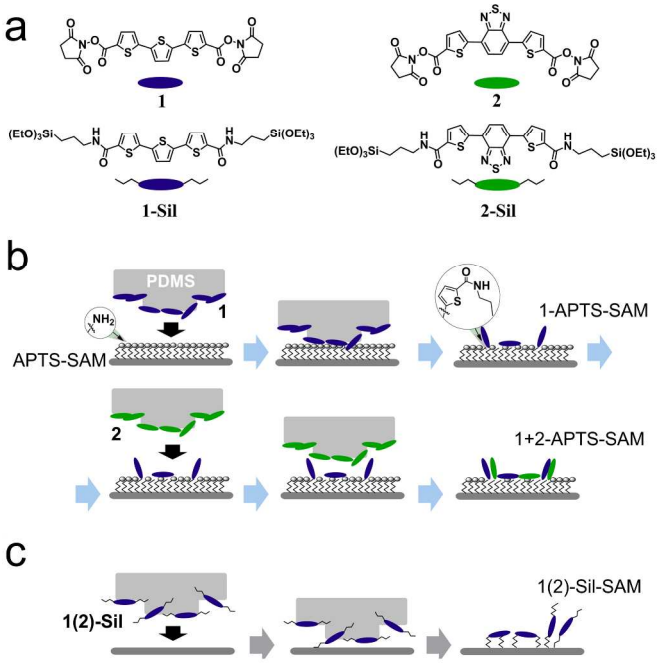


**Figure 1.** a) Molecular structure of all compounds. b). Scheme of the process to fabricate TAG and multi-TAG. Molecule orientations are arbitrary. c) Conventional μCP of **1**-Sil and **2**-Sil on $SiO_2$/Si used to fabricate reference samples.

The scheme of the process is depicted in figure 1b, while figure 1c shows conventional μCP that was exploited to fabricate reference samples starting by triethoxysilane ended **1**-Sil and **2**-Sil already prepared in solution (see ESI). Compounds **1** and **2** were printed on an APTS-SAM by μCP to give **1**-APTS-SAM and **2**-APTS-SAM respectively and were characterized by means of fluorescence microscopy (FM), laser scanning confocal fluorescence microscopy (LSCM), atomic force microscopy (AFM) and X-ray photoelectron spectroscopy (XPS). Figure 2 shows an image of a fluorescent TAG obtained by printing **1** and **2** on APTS- functionalized PDMS, the sample appears transparent and flexible.

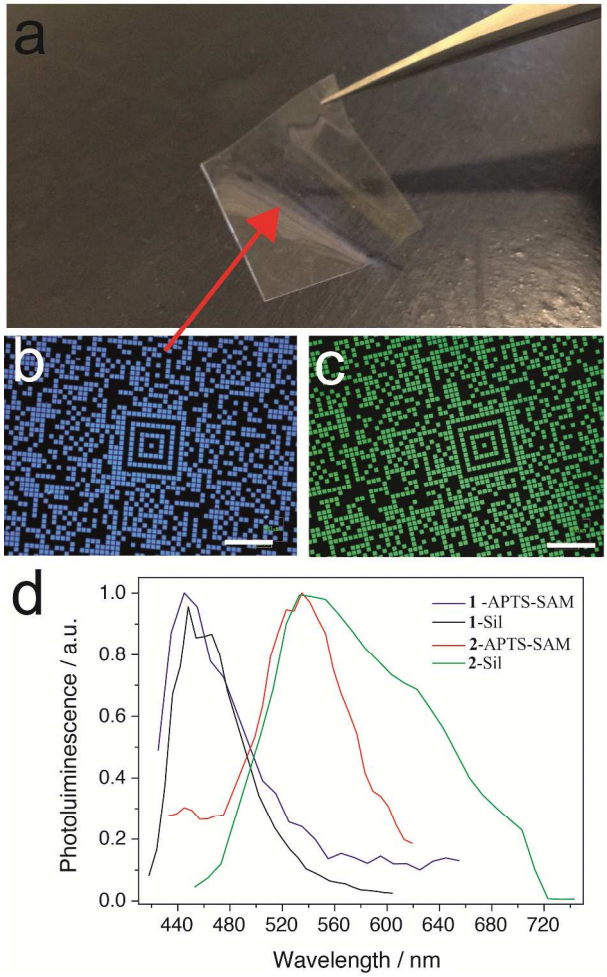


**Figure 2.** a) Photograph of fluorescent TAG obtained on PDMS. b) Fluorescence microscopy images of a portion of **1**-APTS-SAM TAG (bar is 150 μm) and c) **2**-APTS-SAM TAG (bar is 150 μm). d) Normalized confocal spectra of TAGs: **1**-APTS-SAM (blue line), **2**-APTS-SAM (red line), **1**-Sil printed on $Si/SiO_2$ (black line) and **2**-Sil (green line) printed on $SiO_2/Si$.

Figures 2b and 2c show the fluorescence images of two portions of fluorescent TAGs obtained by printing respectively **1** or **2** on APTS-SAM. Both images clearly show high-quality patterns with excellent contrast (An image at fluorescence microscopy of a complete TAG is shown in figure S1). The coverage of compounds can be partially controlled by acting on the concentration of the solution and on the duration of contact, with an upper limit imposed by the saturation of the reactive sites in the SAM or in the surface (see details in ESI). Noticeably, we observed no relevant aging effects for more than 3 months on TAGs stored in air at ambient conditions. Moreover in samples prepared on PDMS no stress effects were observed after bending the TAG to 180° C as a billfold or after stretching it up to 30 % of the length along one direction (effect of stretching are reported in Fig. S2 of ESI). Further stretching beyond this value caused several cracks to appear on the substrate. Exposure of the TAGs to 100 W UV light for more than 1 minute led to photobleaching.

The photophysical properties of the TAGs were investigated with time-resolved and spectral laser scanning confocal fluorescence microscopy. Figure 2d shows the confocal fluorescence spectra of printed TAGs **1**-APTS-SAM and **2**-APTS-SAM compared with TAGs obtained by direct printing of **1**-Sil and **2**-Sil on the bare $SiO_2$ substrate (Fig. 1c), which we used as reference (see ESI).

Printed **1**-APTS-SAM spectrum shows a peak at 445 nm with a shoulder at 475 nm and two fluorescence lifetimes of 0.32 and 1.6 ns, with the short-lived species dominating (Fig. S3)[20, 21]. Both the spectra and lifetimes are almost identical to the spectra and lifetimes of **1**-Sil printed on $SiO_2$ substrate (Fig. 2d and S3-4). The confocal fluorescence spectrum of **2**-APTS-SAM shows a single peak at 535 nm. The fluorescence decay analysis at 585 nm yielded two lifetimes of 6.0 ns and 1.12 ns (Fig. S3); in this case the fluorescence is dominated by the species having the longer lifetime[22]. The spectrum is quite similar to the corresponding spectrum of **2**-Sil directly printed on $SiO_2$ substrate (Fig. 2d). The intense shoulder in the latter spectrum above 580 nm may be indicative of interacting aggregated fluorophores, not observed for **2**-APTS-SAM. So, interestingly μCP of **1** and **2** on APTS-SAM seems preferable to obtain printed SAMs where fluorophores behave mainly independently.

The effective amidic bond formation on the APTS-SAM surface was confirmed by XPS analysis and in particular by N 1s spectrum, which shows two contributions localized at BE = 399.9 eV and 401.6 eV, assigned to amidic and amine groups and their protonated forms (Fig. S4 and Table S1)[23]. Due to the low chemical shift, the assignments were performed by the comparison of N 1s from **2**-APTS-SAM, APTS-SAM and compound **2** (details are reported in ESI). In particular we compared the N 1s signals of three samples (SAM of 2 on Si, 2-compound and APTS on Silicon), as displayed in figure S4 of ESI. The obtained results showed that N 1s signal of compound **2** was characterized by the presence of a component (a'') positioned at BE = 399.2 eV. This component, assigned to the imidic group that is in the succinimidyl end group, disappeared when compound **2** was linked to the Si substrate. In fact, the N 1s signal of the 2-APTS-SAM sample was characterized by two components positioned at BE = 399.8 eV and 401.6 eV, and assigned to amidic and protonated amidic groups, respectively. This result shows that the chemical interaction between compound **2** and APTS-SAM occurred by the transformation of the imidic group to amidic group.

XPS analysis has also been performed to estimate the thickness of the organic layer (i.e. **2**-APTS SAM). This was carried out by collecting photoelectrons at the take-off angle of 60° with respect to its normal (fig. 3), increasing the surface sensitivity[24]. The thickness was calculated by using the Avantage v.5 software. The calculation reveals a total thickness of the organic layer (APTS + compound) of about 0.7 nm that considering the length of APTS (0.54 nm)[25] results in an estimated thickness of printed compound of 0.16 nm, which is comparable with the thickness obtained by AFM (see ESI and Fig.S5).

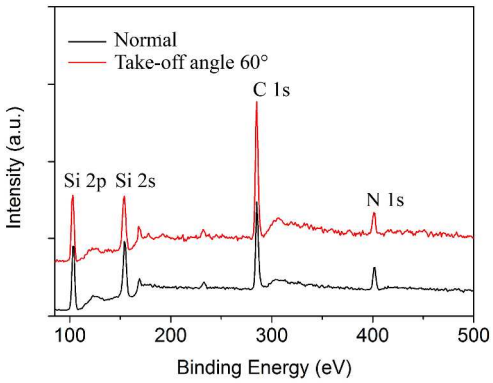


**Figure 3.** Angle resolved XPS analysis for the estimation of the thickness of the organic layers. Comparison of survey spectra acquired on the sample positioned normal (black line) and tilted of 60° (red line) respect to the analyzer.

AFM topographic imaging of TAG revealed a series of clear marks from both μCP iterations (Fig. 4b).

While the outlines of the individual printed areas are clearly distinguishable from the APTS background (possibly due to a different organization of the compounds in these borderline areas, or to a limited material accumulation attributable to the corner effect),[26-28] the average heights of unprinted, singly, and printed areas were found to be identical, within experimental error (see Fig. S5 and ESI). Root mean squared area roughness ($S_q$) values of unprinted, singly-printed, and multi-printed areas were also undistinguishable (Sq = 0.3 ± 0.1 nm in both cases).

Taken together, these experimental observations suggest that, as the **1-2** soaked stamp is placed in contact with the APTS-SAM, the succinimidyl-ester end groups react with the exposed -$NH_2$ moieties of the SAM. The corresponding amides linked molecules are mainly oriented parallel to the surface, this meaning that probably both succinimdyl end groups react with the SAM, except a few molecules at the boundaries of printed zones, where they can adopt different orientations. The covalent bonds at surface prevent any molecular aggregation and reorganization during the post printing treatment.

In order to prove the possibility to render the process additive, we printed in the same area compounds **1** and **2** by two independent printing steps (Fig. 1b and Fig. 3a) to fabricate a so named multi-TAG.

The multi-TAG shows square areas containing single compounds (1 or 2) or both interpenetrating compounds (1+2) (Fig. 4a,b). In the clearly distinguishable areas in which only one compound is present we observe a photophysical behavior identical to that of the TAG of the single compounds, **1**-APTS-SAM and **2**-APTS-SAM where fluorophores behave independently. In the areas where both compounds are present (**1+2**-APTS-SAM), the confocal spectroscopic measurements are indicative of a summed spectrum of the two separate compounds (Fig. 4e), even though the fluorescence intensities of both **1** and **2** is somewhat lower in these mixed areas (see intensity profiles in ESI, Fig. S6). One reason for the lower intensity observed for **1,** printed first, may be energy transfer from compound **1** to **2** in close proximity. To check this hypothesis, we analyzed the fluorescence decay for emission at 480 nm in the mixed areas. The fluorescence lifetimes of 0.29 and 2.44 ns for compound **1** are unaltered compared to the single **1**-APTS-SAM TAG and do not unequivocally prove energy transfer (Fig. S7 and table S2)[29]. On the other hand for compound **2**, the lower fluorescence intensity may be due to the fact that it is deposited during the second printing step, in which a smaller number of reactive amino sites are available. Apart from this, the shortening of the lifetimes to 0.80 and 4.44 ns observed analyzing the decay of photons collected at 585 nm in the mixed areas (Fig. S7 and table S2, S3) could be likely ascribed to an electron transfer process between compound **1** and the more electron deficient **2**. So in the mixed area we do not exclude some possible interaction between some fluorophores in close proximity. Noticeably, in the multi-TAG the contribution of each single TAG can be simply distinguished by selecting the opportune emission channel in LSCM (Figs. 4c,d) or using different filters in fluorescence optical microscope (Fig. S8). As in the case of single TAG the average heights of unprinted, singly, and doubly-printed areas were found to be identical, within experimental error (Sq = 0.3± 0.1 nm in all cases, see fig. S8 and ESI).

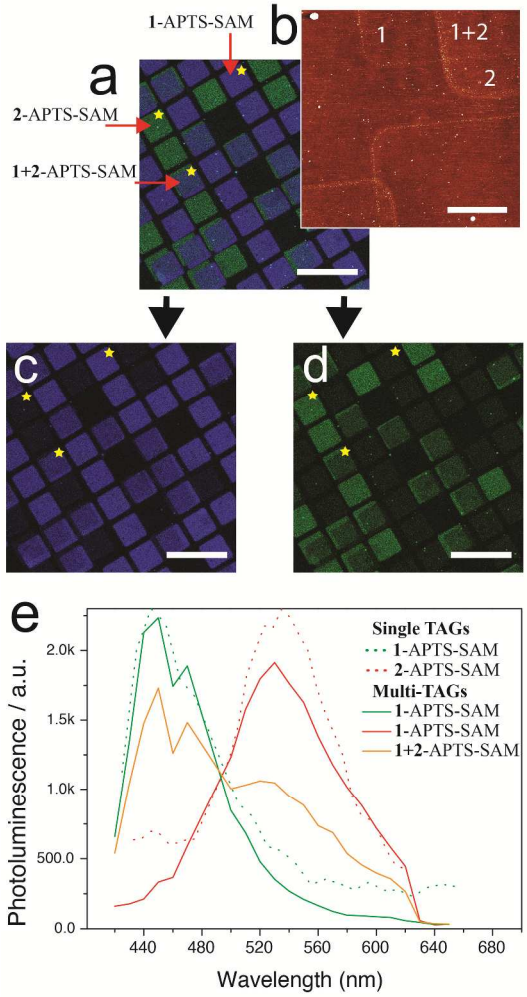


**Figure 4.** Confocal fluorescence images of multi-TAG, recording emission at 450 and 520 nm with laser excitation at 405 nm.
a) overlay of both channels; bar is 20 μm, the stars are guide for eyes, b) Corresponding AFM image (scale bar: 5 μm, Z scale: 0-5 nm) the numbers inside the figure indicate the places were only one (**1, 2**) or both (**1+2**) compounds are printed. c). Multi-TAG emission at 450 nm. d) Multi-TAG emission at 520 nm. e) Comparison of confocal spectra for specific zones of the multi-TAG (lines) and TAG (dotted lines). **1 (2)**-APTS-SAM areas containing the isolated fluorophores **1** (green line) or **2** (red line), **1+2**-APTS-SAM areas, of the same size, containing both compounds interpenetrated (orange line). The spectra of single TAG are normalised.

The possibility to independently read the different contribution of each compound of the multi-TAG offers a great technological advantage since not fine alignment is required for the process (in our experiments the rough alignment is obtained under an optical microscope using some markers present in the stamp).
Summarizing the available information on molecular arrangement of printed molecules: FM and LSCM spectra show that both species have homogeneous structures in terms of both fluorescence intensity and spectral shape, which is moreover very similar to the spectra obtained in diluted solution (Fig. S9). XPS measurements show the **1**,**2**-APTS bond formation, while AFM shows a mean thickness less than 0.3 nm (except on the boundaries). The fluorescence lifetime of printed features is quite similar to those of the compounds in diluted solution, and XPS does not show evidence of aggregation.

## Conclusions

In conclusion, reiterated μCP has been used to reliably fabricate a fluorescent micrometric multi-TAGs consisting of two interpenetrated logic pattern made of two different fluorescent compounds on a R-SAM both on rigid and flexible substrates. The first printing step deposits an amount of molecules that does not lead to complete saturation of the amino-groups of APTS-SAM, leaving reactive sites available for a second μCP iteration. From a fundamental point of view, we prove that different molecules can additively functionalize R-SAMs, preserving largely the individual photophysical properties of the single grafted molecules. In this respect, our work represents an important advance in view of the application of reactive and SAMs in nanotechnology.
Here, we used **1** and **2** compounds on APTS-SAM as representative materials because they are easily detectable by optical microscopy, but, considering the number of compounds ended with amino-reactive group, we are confident that the process could be extended to many other functional materials. In principle, the process can be extended to "reversible" SAMs such as alkanethiol SAMs. In forthcoming work, the resolution of the patterning process can be scaled further down to smaller scales. In addition, the use of more than two molecules and the combination of more functionality by using additive, modular functionalization can be envisioned. This on-going work might lead to the development of a new generation of devices, for instance storage media based on a variety of optical responses and sensors.

## Acknowledgements

We thank Francesco Valle for fruitful discussions. The activity has been supported by national Project N-CHEM, Flagship NANOMAX and ESF-EuroBioSAS ICS.

## Notes and references

[a] Istituto per lo Studio dei Materiali Nanostrutturati
Consiglio Nazionale delle Ricerche- Via P. Gobetti 101, 40129 Bologna and Via Salaria km 29,3 00015 Monterotondo, Roma, IT.
E-mail: massimiliano.cavallini@cnr.it
[b] Istituto per la sintesi Organica e la Fotoreattività
Consiglio Nazionale delle Ricerche, Via P. Gobetti 101, 40129 Bologna.
[c] Scriba Nanotechnologie S.r.l. Via di Corticella 183/8 40128 Bologna, IT.

† DG and MB contributed in the same manner to this work.

Electronic Supplementary Information (ESI) available: [Experimental details, synthesis and characterization of compounds **1**, **2**, **1**-Sil and **2**-Sil, materials are described in the supporting information.]. See DOI: 10.1039/c000000x/

1. N. Crivillers, S. Osella, C. Van Dyck, G. M. Lazzerini, D. Cornil, A. Liscio, F. Di Stasio, S. Mian, O. Fenwick, F. Reinders, M. Neuburger, E. Treossi, M. Mayor, V. Palermo, F. Cacialli, J. Cornil and P. Samorì, *Adv. Mater.*, 2013, 25, 432-436.
2. X. Y. Cheng, Y. Y. Noh, J. P. Wang, M. Tello, J. Frisch, R. P. Blum, A. Vollmer, J. P. Rabe, N. Koch and H. Sirringhaus, *Adv. Funct. Mater.*, 2009, 19, 2407-2415.
3. D. Astruc, E. Boisselier and C. Ornelas, *Chem. Rev.*, 2010, 110, 1857-1959.
4. E. Hutter and J. H. Fendler, *Adv. Mater.*, 2004, 16, 1685-1706.
5. M. Melucci, M. Zambianchi, L. Favaretto, V. Palermo, E. Treossi, M. Montalti, S. Bonacchi and M. Cavallini, *Chem. Commun.*, 2011, 47, 1689-1691
6. D. Gentili, G. Foschi, F. Valle, M. Cavallini and F. Biscarini, *Chem. Soc. Rev.*, 2012, 41, 4430-4443.
7. M. Cavallini, R. Lazzaroni, R. Zamboni, F. Biscarini, D. Timpel, F. Zerbetto, G. J. Clarkson and D. A. Leigh, *J. Phys. Chem. B*, 2001, 105, 10826-10830.
8. C. Menozzi, V. Corradini, M. Cavallini, F. Biscarini, M. G. Betti and C. Mariani, *Thin solid films*, 2003, 428, 227-231.
9. P. Leclere, M. Surin, R. Lazzaroni, A. F. M. Kilbinger, O. Henze, P. Jonkheijm, F. Biscarini, M. Cavallini, W. J. Feast, E. W. Meijer and A. Schenning, *J. Mater. Chem.*, 2004, 14, 1959-1963.
10. X. Yao, Y. L. Song and L. Jiang, *Adv. Mater.*, 2011, 23, 719-734.
11. M. Cavallini, G. Aloisi, M. Bracali and R. Guidelli, *J. Electroanal. Chem.*, 1998, 444, 75-81.
12. L. Netzer and J. Sagiv, *J. Am. Chem. Soc.*, 1983, 105, 674-676.
13. A. Ulman, *Chem. Rev.*, 1996, 96, 1533-1554.
14. M. Cavallini, M. Bracali, G. Aloisi and R. Guidelli, *Langmuir*, 1999, 15, 3003-3006.
15. Y. N. Xia and G. M. Whitesides, *Angew. Chem., Int. Ed.*, 1998, 37, 551-575.
16. M. Geissler and Y. N. Xia, *Adv. Mater.*, 2004, 16, 1249-1269.
17. C. Nicosia and J. Huskens, *Materials Horizons*, 2014, 1, 32-45.
18. L. Yan, X. M. Zhao and G. M. Whitesides, *J. Am. Chem. Soc.*, 1998, 120, 6179-6180.
19. M. Cavallini, A. Calo, P. Stoliar, J. C. Kengne, S. Martins, F. C. Matacotta, F. Quist, G. Gbabode, N. Dumont, Y. H. Geerts and F. Biscarini, *Adv. Mater.*, 2009, 21, 4688-4691.
20. N. DiCésare, M. Belletête, A. Donat-Bouillud, L. Mario and G. Durocher, *J. Lumin.*, 1999, 81, 111-125.
21. D. Anestopoulos, M. Fakis, G. Mousdis, V. Giannetas and P. Persephonis, *Synth. Met.*, 2007, 157, 30-34.
22. J. Pina, J. S. de Melo, D. Breusov and U. Scherf, *Phys. Chem. Chem. Phys.*, 2013, 15, 15204-15213.
23. R. A. Shircliff, P. Stradins, H. Moutinho, J. Fennell, M. L. Ghirardi, S. W. Cowley, H. M. Branz and I. T. Martin, *Langmuir*, 2013, 29, 4057-4067.
24. M. P. Seah and D. Briggs, *Practical Surface Analysis*, 1992.
25. G. Demirel, G. Birlik, M. Cakmak, T. Caykara and S. Ellialtioglu, *Surf. Sci.*, 2007, 601, 3740-3744.
26. M. Cavallini, D. Gentili, P. Greco, F. Valle and F. Biscarini, *Nat. Protoc.*, 2012, 7, 1569-1764.
27. M. Cavallini, M. Facchini, M. Massi and F. Biscarini, *Synth. Met.*, 2004, 146, 283-286.
28. M. Cavallini, *J. Mater. Chem.*, 2009, 19, 6085-6092.
29. Note: shortening of the dominating lifetime of 0,29 ns, observed for the single compound TAG of compound **1**, would have led to a lifetime that is below the time resolution limit of our instrumental setup, so we may not observe lifetime shortening that occurs due to energy transfer from **1** to compound **2**.



 